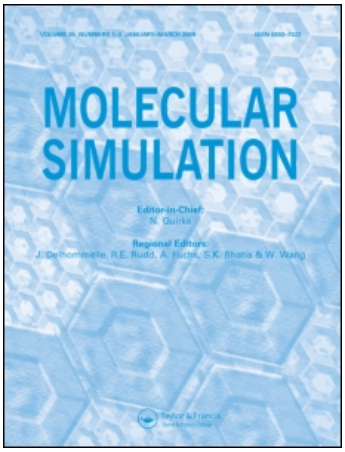

Molecular Simulation
Publication details, including instructions for authors and subscription information:
http://www.informaworld.com/smpp/title~content=t713644482

Modeling of Proton Transfer in Polymer Electrolyte Membranes on Different Time and Length Scales

P. Commer[a]; C. Hartnig[a]; D. Seeliger[a]; E. Spohr[a]
[a] Institut für Werkstoffe und Verfahren der Energietechnik (IWV-3), Jülich, Germany

Online publication date: 26 October 2010

To cite this Article Commer, P. , Hartnig, C. , Seeliger, D. and Spohr, E.(2004) 'Modeling of Proton Transfer in Polymer Electrolyte Membranes on Different Time and Length Scales', Molecular Simulation, 30: 11, 755 — 763
To link to this Article: DOI: 10.1080/0892702042000270179
URL: http://dx.doi.org/10.1080/0892702042000270179

Molecular Simulation, VOL. 30 (11–12), 15 September–15 October 2004, pp. 755–763

Taylor & Francis
Taylor & Francis Group

Modeling of Proton Transfer in Polymer Electrolyte Membranes on Different Time and Length Scales

P. COMMER, C. HARTNIG, D. SEELIGER and E. SPOHR*

Institut für Werkstoffe und Verfahren der Energietechnik (IWV-3), Forschungszentrum Jülich, D-52425 Jülich, Germany

(Received November 2003; In final form March 2004)

Polymer electrolyte membranes (PEMs) are key component materials in fuel cell technology. Understanding the relationship between the elementary acts of proton transport and the operation of the entire cell on different time and length scales is therefore particularly rewarding. We discuss the results of recent atomistic computer simulations of proton transport in porous PEMs. Different models cover the range from individual local proton hops to diffusion processes with polymer mobility included.

Keywords: Polymer electrolyte membrane; Proton transfer; Molecular dynamics; Computer simulation; Fuel cell

INTRODUCTION

Fuel cells are considered as one of several environmentally beneficial alternatives for energy conversion. Their function is based on the spatial separation of oxidation and reduction steps in an exothermic combustion reaction such as

$$H_2 + \frac{1}{2}O_2 \rightarrow H_2O$$

or

$$CH_3OH + \frac{3}{2}O_2 \rightarrow CO_2 + 2H_2O.$$

The heart of the fuel cell is formed by the electrolyte, which separates anode and cathode regions and mediates the electrochemical reactions by specifically transporting one ion at a very high rate. In high temperature fuel cells, the electrolyte is usually a solid oxide with high oxygen ion conductivity. In low temperature fuel cells (see, e.g. Refs. [1–3] for an overview), the electrolyte is a proton-conducting polymer membrane.

For reasons of mechanical and thermal stability as well as stability towards strong acids and oxidative environments, the class of polymer electrolyte membranes (PEMs) which are currently employed in fuel cell applications consists, in most cases, of polytetrafluoroethylenes with SO_3^- -terminated perfluorinated side chains (such as Nafion®, Dow®, and Asahi membranes) or stochastically sulfonated polymeric phenylene–ether–keto compounds (such as PEK, PEEK, PEEKK etc.).

The output of electrical power of a low temperature fuel cell strongly depends, among other factors, on the rate at which protons migrate through the PEM under operating conditions. The performance of the entire fuel cell system is closely related to the distribution of water in the cell ("water management") and, for the direct methanol fuel cell (DMFC), to the minimization of methanol crossover. Both problems arise as a consequence of the membrane's permeability for small molecules and of electro-osmotic co-transport of solvent molecules with protons. Understanding the molecular details of proton transport (PT) in such materials is thus of paramount importance for the development and improvement of materials. The overall function of a PEM depends on a number of molecular processes with different characteristic time and length scales. Modeling techniques can aid our understanding on each of these different scales.

In the next section, we discuss in detail the role of these different scales for proton conductance from the anode, where they are created, through the membrane to the cathode, where they are consumed.

*Corresponding author. E-mail: e.spohr@fz-juelich.de

ISSN 0892-7022 print/ISSN 1029-0435 online © 2004 Taylor & Francis Ltd
DOI: 10.1080/0892702042000270179

We focus on results of (atomistic) molecular dynamics (MD) computer simulations, which have been performed to investigate molecular processes on several of these scales. This is followed by a discussion of some necessary future steps to generate a complete picture of PT in a rather complex non-equilibrium system such as a fuel cell membrane.

PROTON TRANSPORT IN POLYMER ELECTROLYTE MEMBRANES

Proton Hops

PEM materials can take up a significant amount of water. Because of their nonpolar main chain and polar SO_3^- head group aqueous and polymeric regions separate on the nanometer scale. A bicontinuous material is formed with the polymeric phase providing structural stability and the aqueous phase providing the environment for PT [4–6]. In Nafion, this hydrophilic/hydrophobic nano-separation occurs spontaneously already in the dry state [7]. The aqueous regions are large enough to contain solvated proton clusters $H_{2n+1}O_n^+$. The smallest possible clusters are the hydronium ion H_3O^+ and the Zundel ion $H_5O_2^+$. Thus, like in bulk aqueous solutions, proton transfer can occur either via normal diffusive processes of the protonated water cluster as an entity or via a hopping mechanism in which one proton is transferred from an H_3O^+ ion to a neighbouring H_2O molecule, which is followed by transfer of (usually) a different hydrogen atom of the newly formed H_3O^+ to another H_2O neighbour. Thereby charge transport is not combined with mass transport. This so-called *Grotthus* or relay mechanism [8,9] is the dominant contribution to proton mobility in aqueous acids; it is responsible for the significantly higher proton mobility as compared to simple alkali ions with sizes similar to the hydronium ion. The role of this mechanism in bulk aqueous systems was elucidated by recent *ab initio* molecular dynamics simulations using the Car-Parrinello method based on gradient-corrected density functional theory [10–15]. Characteristic rates of proton hops are of the order of $1\,ps^{-1}$. At that rate, individual protons are moved along the O—H—O axis by about 0.4 Å, while the center of charge moves about 2.4 Å.

The relay mechanism manifests itself in concentrated acids not only as a large magnitude of the proton mobility but also as weak temperature dependent with a low activation energy of $E_a = 0.107\,eV$ [16]. Proton transport in PEMs such as Nafion shows similar characteristics: at high water content of the membrane, proton conductivity can be high (about $0.1\,S\,cm^{-1}$), and the activation energy can be similar to that in bulk acids. Only when the water content in the membrane is reduced, proton conductance decreases and the activation energy increases [17].

PEM conductance properties can be modelled atomistically under realistic (water-rich) conditions only if one takes into account the relay mechanism of the individual proton hops. This requires in an MD simulation, the integration of the equations of motion on a smaller time scale than for the normal diffusion mechanism, which makes the calculations more demanding in terms of CPU resources. An obvious choice of modelling paradigm would be the use of *ab initio* simulation methods similar to those used for the bulk, since they can adequately describe the formation and breaking of chemical bonds during the proton hop. Unfortunately, the computational expense makes the methods unusable for large systems such as polymer/water mixtures, and this approach has not been used so far to investigate PT in PEMs. It has, however, been applied to the study of crystal hydrates of simple model compounds, which contain only few essential aspects of Nafion chemistry and only a single proton [18,19]. These calculations were extended by the same authors to investigate more than one proton in a study of the role of crystalline defects in a crystal of $4\,H_3O^+\cdots CF_3SO_3^-$ entities [20]. A more realistic model of the polymer/aqueous interface, where the spacing between sulfonic acid groups is larger, would require an even larger number of atoms.

Recently, significant work on the feasibility of so-called empirical valence bond (EVB) models for the description of nonclassical proton transfer has been performed [21–29]. The method describes the state of a supra-molecular system as a linear combination of VB states $|\psi_i\rangle$,

$$|\Psi\rangle = \sum_i a_i |\psi_i\rangle, \tag{1}$$

with $\langle \Psi|\hat{H}|\Psi\rangle$ the expectation value of energy. Unlike VB theory in quantum mechanics, the matrix elements of the Hamiltonian $\hat{H}$ are not calculated in an electronic basis but by empirical force fields. As an example, the $H_5O_2^+$ complex can be described as a superposition of two states $|\psi_1\rangle$ and $|\psi_2\rangle$, namely $H_2O{-}H^+\cdots H_2O$ and $H_2O\cdots H^+{-}OH_2$ (here, — describes a chemical bond and ⋯ a hydrogen bond). The energy of each state is calculated from empirical force field terms for intramolecular hydronium interactions, intramolecular water interactions and for the intermolecular water-hydronium interactions, yielding H_{11} and H_{22}. The energy of the two states is, in general, non-identical. By further specifying empirical coupling functions $H_{12}(\{q\}) = H_{21}(\{q\})$ as functions of the set of particle coordinates $\{q\}$, the compound states can be calculated via diagonalization of the Hamiltonian

matrix [30]. With the additional approximation that all atoms move classically on the (time-dependent) ground state potential energy surface a viable MD scheme can be developed. The procedure is analogous for larger clusters with more basis states.

Proton transfer dynamics can be described with such a scheme, when the selection of contributing basis states (i.e. water molecules) can change over time. In this case, care has to be taken that new basis states (water molecules) are added to the cluster already at a time when their contribution to the ground state is still negligibly small and, similarly, basis states can only be removed when their contribution has already become negligible. Otherwise, the trajectory of the system will not conserve total energy.

One possible consequence is that a large number of basis states, say 20, is used, which is equivalent to a proton cluster $H_{41}O_{20}^{+}$ in which, however, the contributions of some states are negligible at any given time. While this can be done with good success for single protons [22,24,28], a problem arises when the proton concentration becomes large: in this case, some water molecules can contribute to more than one state and thus the proton Hamiltonians cannot be diagonalized individually anymore, leading to significant computational overhead for the calculation of the EVB states. Therefore, Walbran and Kornyshev [29] chose a different route. In their simplified EVB model of the Zundel ion only two VB basis states per proton are needed and PT is described as a series of individual Zundel → Hydronium and Hydronium → Zundel ion conversions. The model involves an explicit dependence of the partial charges (or, more generally speaking, some potential parameters) on the local coordinates of the Zundel complex, which simplifies the calculation of Coulomb interactions significantly by avoiding the diagonalization procedure of larger matrices (in the worst case, a $2^N \times 2^N$ matrix, where N is the number of protons involved). Yet this comes at the expense of adding an extra force term (see Ref. [29] for more details). The coupling elements $H_{12} = H_{21}$ are chosen in such a way, that at any time they can be non-zero only for at most one H_2O neighbour of a H_3O^+ entity, due to geometric constraints. Thus, at any time the proton transfer cluster is uniquely defined. If H_{12} (temporarily) vanishes, the Zundel ion cluster can be reassembled by selecting another H_2O molecule to enter the cluster. This approach has been used in our group for modeling PT in pores of typical PEM materials (see, Refs. [31,32], and below).

The rate of proton hops in PEMs is not so much influenced by the overall structure of the water/polymer two-phase system but rather by local properties, such as density of sulfonate (SO_3^-) groups and water content in the vicinity of the transferring protons and, of course, temperature. Local motions of sulfonate head groups and (less likely) side chains (in Nafion-like materials) may influence the proton transfer rate via fluctuation-assisted barrier reduction due to fluctuations in the electrostatic potential; however, the transport does not depend much on slow changes in pore arrangement. Thus, for a first approach it is reasonable to focus on individual pores.

Therefore, slab and cylinder models of single pores were developed [31,32], in which a smooth wall models the main chain and the side chain of the polymer. In such pore models, the surfaces are decorated with (static or mobile) SO_3^- groups at varying surface density. Water content is varied by changing the number of water molecules (and thus the thickness) of the slab pore. Such a simplified model allows for the calculation of statistically reliable proton jump rates and diffusion coefficients (parallel to the slab surface) by averaging over several thousand proton jumps, which corresponds to simulation times in the range of nanoseconds. For these simulation times the cpu time requirements are such that systematic variations of operational parameters of a fuel cell can be performed. Among them are water content, temperature and polymer properties like the acid strength (which is related to the delocalization of the anion charge into the polymer chain) or the density of SO_3^- groups, which is inversely proportional to the equivalent weight (the molecular weight of polymer per SO_3^- group).

Figure 1 demonstrates how the proton hopping rate is related to the diffusion coefficient. The figure shows data from slab pores, the smooth pore surfaces of which are decorated with mobile SO_3^- groups, which are tethered to the equilibrium sites of a square lattice with given surface density (see Ref. [32] for details). The diffusion coefficient D parallel to the pore surface is calculated using the Einstein

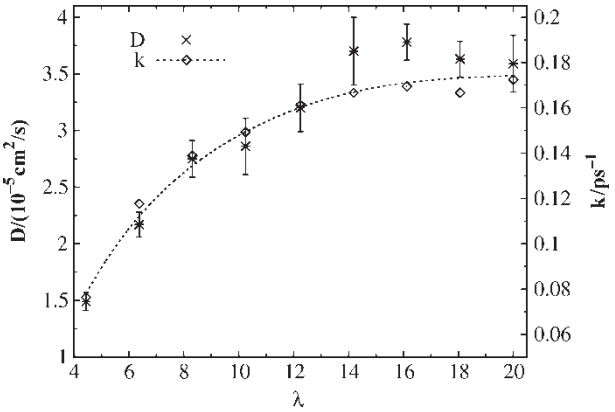

FIGURE 1 Self diffusion coefficient D (×, left axis) and rate constant k for proton transformations (◆ with dashed line, right axis) as a function of water content $\lambda = n_O/n_{H+}$ (oxygen-to-proton-ratio) from simulations of a smooth-walled slab whose walls are decorated with tethered SO_3^- groups of a surface density of $(1/58)\text{Å}^{-2}$. See text for further details.

relation in two dimensions for the center of charge of the Zundel complex. For the same systems rate constants k have been calculated for the rate of "long" $H_3O^+ \rightarrow H_3O^+$ and $H_5O_2^+ \rightarrow H_5O_2^+$ transfers (see also Ref. [33]). What is called a "long" transfer here is in fact a sequence of two $H_5O_2^+ \rightarrow H_3O^+ \rightarrow H_5O_2^+$ or $H_3O^+ \rightarrow H_5O_2^+ \rightarrow H_3O^+$ transitions, such that none of the oxygen atoms of the final cluster were part of the initial one. For the $H_3O^+ \rightarrow H_3O^+$ jumps, we monitor the time it takes between the formation of a given H_3O^+ ion and the formation of a new H_3O^+ ion whose oxygen atom is not one of the original nearest neighbours of the first oxygen atom. Similarly, for "long" $H_5O_2^+ \rightarrow H_5O_2^+$ we monitor the time it takes from the formation of a $H_5O_2^+$ ion to the formation of a new one with two different oxygen atoms. The rate constant k is obtained by averaging the inverse times over all events. Regarding temperature dependence, these transfer rates were found to correlate better with the diffusion coefficient in bulk water than the corresponding "short" transfer rates, which involve only one $H_5O_2^+ \rightarrow H_3O^+ \rightarrow H_5O_2^+$ or $H_3O^+ \rightarrow H_5O_2^+ \rightarrow H_3O^+$ step (see discussion in Ref. [33]). The diffusion coefficient and the rate constant show a similar dependence on water content $\lambda = n_O/n_{H+}$ (oxygen-to-proton ratio). The contribution of non-classical (Grotthus) proton transport to proton mobility is thus largely independent of water content in the simulated simple PEM pores. Hence, local proton hopping on the picosecond time scale significantly determines the simulated proton diffusion and conductivity even at low water content. From experimental data [34] one can, however, conclude that the relative importance of the Grotthus mechanism for proton diffusion decreases with decreasing water content.

Activation Energy of Proton Diffusion in Single Model Pores

Figure 2 shows the temperature dependence of diffusion coefficients D and rate constants k in Arrhenius representation for two different water contents i.e. $\lambda = 5.4$ describes a pore in a dry membrane, while $\lambda = 12.3$ corresponds to a pore in a (swollen) humid membrane as it might occur in polymer electrolyte membrane fuel cells during operation. Considering the PT as an activated process,

$$D, k \sim \exp(-E_a/k_B T), \tag{2}$$

the activation energies E_a for proton transition and diffusion are very similar for both water contents. This indicates, as mentioned above, that diffusion is strongly associated with proton transformations of the Grotthus type. Furthermore, the activation energies are almost identical for the two different values of λ.

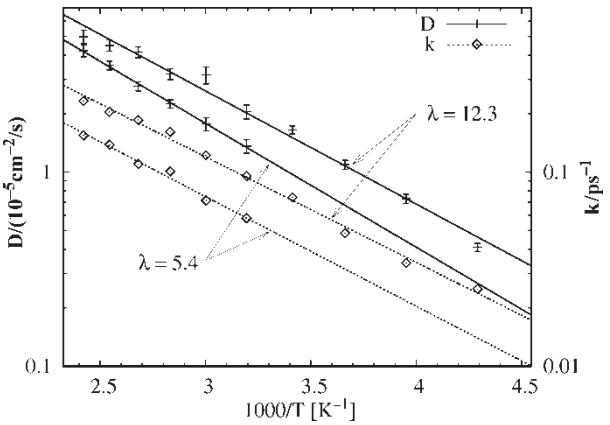

FIGURE 2 Temperature (T) dependence of diffusion coefficient D (full lines, left axis) and rate constant k for proton transformation (dashed line, right axis) in Arrhenius representation. Data are taken from simulations of a smooth-walled slab whose walls are decorated with tethered SO_3^- groups of a surface density of $(1/58)\text{Å}^{-2}$ at two different water contents λ as indicated.

Experimental observations indicate that proton conductance increases with water content at fixed temperature T [1]. Furthermore, the activation energy depends on water content λ in such a way that the activation energy for water-rich membranes approaches the corresponding value in bulk acids but increases in very dry membranes [17]. A simple model based on Poisson–Boltzmann theory [35] rationalized the experimental results for the *membrane* conductance by an analysis of the proton distribution and Coulomb barriers for diffusion in a *single pore*. According to this model, proton mobility in very narrow pores is dominated by protons in close proximity to the SO_3^- groups which have a higher barrier for individual proton hops due to the additional Coulomb barriers produced by these groups. Proton mobility in water-rich pores, on the other hand, is dominated by Grotthus transport with negligible contributions from events with high activation energy near the pore surfaces.

Figure 2 and other simulation results [32] as well as more realistic modifications of Poisson–Boltzmann theory (which are discussed in some detail in Ref. [32]), however, show that the mechanism of proton mobility in the single pore does not depend strongly on the *local water content* in an isolated pore. The simulated activation energies are almost constant. The fact that the activation energies of the rates of "long" proton hops is rather similar to the activation energy of diffusion underlines the important role of local proton hops for diffusional motion at all temperatures (see also previous subsection).

The discrepancy to the experimental observation may have various reasons. First and foremost, the calculations discussed here are for a single pore. Real membranes consist of a pore network with a wide distribution of pore sizes and forms. Particularly at low membrane water content, the very narrow pores

and their percolation properties may determine the conductance. In such a situation a gating step in which pore connections open and close might become rate determining. Such a step has been conjectured by Vishnyakov and Neimark [36] on the basis of simulations of the potassium form of Nafion 1200. Since a gating step is likely to involve a large number of degrees of freedom one can only speculate whether such a step would involve activation energies significantly larger than the experimentally observed ones.

Influence of some Chemical and Physical PEM Properties

The simple slab pore models can also be used to investigate some generic chemical and physical properties of different PEM materials. Such materials are different with respect to where the acidic groups are located (on side chains as in Nafion and related materials or on the main chain such as PEEK and others) and the side chain length. These properties determine to a significant extent the local mobility of the SO_3^- groups. Furthermore, the acid strength of the individual SO_3H group and the degree of sulfonation determine the concentration of protons in the pore and thus the pH as well as the conductivity.

In Ref. [31] we investigated these effects in detail; the model used includes only the head groups without any fluorinated side chain or main chain. There it was concluded that counter-charge delocalization (i.e. acid strength of the SO_3H group) is the most important factor to speed up proton mobility in a pore. Acid strength was modelled by simulating different partial charge distributions for the SO_3^- ion. More elaborate quantum chemical calculations of crystal hydrates by Paddison *et al.* [18,19] show how chemical modifications of side chain entities can make dissociation of the acid more complete.

Sulfonate head group mobility was also found to influence proton transport in two ways. In the model, sulfonate groups are tethered through the S atom to equilibrium positions on the pore surface. One effect is that librational motion of the sulfonate group around its symmetry axis leads to effective charge delocalization at the position of the individual SO_3^- groups. In addition, the increased fluctuations in electrostatic potential due to lateral position fluctuations of SO_3^- groups on the pore surface can lead to a fluctuation-assisted reduction of the Franck-Condon barriers (see Ref. [31]).

Figure 3 shows the influence of the PEM's equivalent weight on the proton diffusion coefficient. Each curve reflects the general experimental trend that proton mobility is low at low water content and increases to some saturation value with increasing water content (see also Fig. 1). With increasing SO_3^- density, the mobility of individual protons decreases.

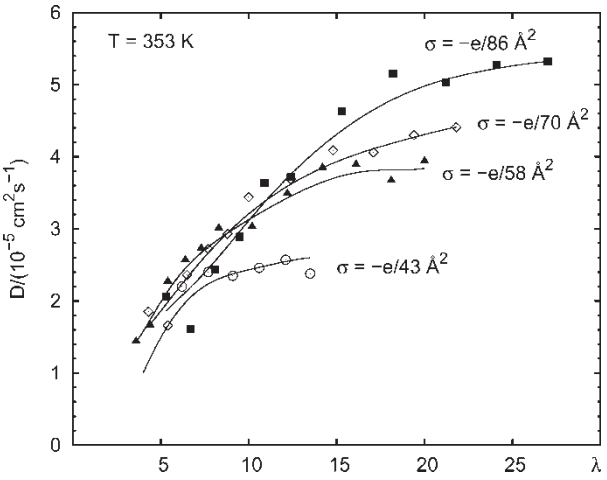

FIGURE 3 Proton self diffusion coefficient D for slab pores as a function of the oxygen-to-proton ratio λ for four different values of the surface charge density σ, corresponding to the mean area per SO_3^- group as indicated. e is the elementary charge. Results are taken from several series of simulations with tethered sulfonate ions on the slab surface.

The reason for this behavior lies in the fact that the distribution of protons (see the density profiles in Fig. 4) near the pore surface is the more localized the higher the charge density is; this is in line with the predictions of simple Gouy-Chapman theory that the width of the diffuse ionic layer near a charged surface decreases with increasing surface charge density. Assuming the validity of the Nernst relation (thus excluding coupling effects between protons) and neglecting the small contribution from the SO_3^- groups, the conductance of the membrane is proportional to the product of proton diffusion coefficient and concentration. With these assumptions, the conductance of a pore increases with increasing equivalent weight (due to concentration increase) as well as with increasing water content, in qualitative agreement with the experimentally observed trends [1].

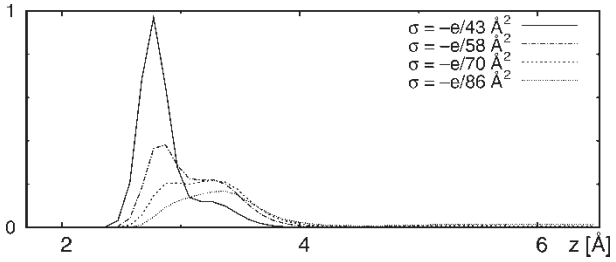

FIGURE 4 Proton density distribution near the pore surface for pores with $\lambda = 8.3$ for four different values of the surface charge density σ, corresponding to the mean area per SO_3^- group as indicated. z is the distance of the center of proton charge from the pore surface. Results are taken from simulations with tethered sulfonate ions on the surfaces of the slab surface.

Influence of Nafion Side Chains on PT Dynamics

The above slab models employed only SO_3^- head groups and completely neglected main chain motion and, in Nafion, side chain motion. Side chain motion has been incorporated into the slab model by simulating slabs with smooth walls onto which entire Nafion side chains

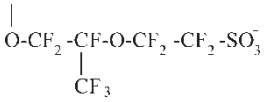

have been tethered via the first ether-oxygen atom [31,37]. Slabs with side chains show a higher proton mobility than slabs with sulfonate groups directly attached to the smooth wall. The simulations did not last long enough to show the effect of large conformational changes. Nevertheless, they include the influence of conformational disorder. As a consequence, the proton distribution in those pores is more homogeneous than in the pores with head groups only.

In order to separately investigate side chain motion and conformational disorder in more detail, simulations of the Nafion/water two-phase systems have been started [38]. In these simulations, the rigid SPC/E water model [39] and the rigid hydronium model of Fornili *et al.* [40] have been used together with a rigid-bond version of the Nafion model (using the same interaction parameters as those given in Ref. [31], but with equilibrium bond length constraints). The rigidity of the model allows larger time steps of up to 2.5 fs and thus allows the simulation on a time-scale in excess of 20 ns for the all-atom case. Figure 5 shows the time-dependence of the dihedral angle θ around the C—C bond as indicated in the inset. Different torsion angles

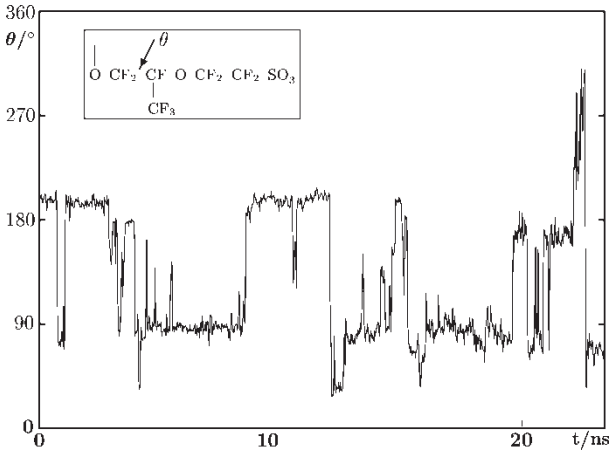

FIGURE 5 Time dependence of the torsion angle θ in one specific Nafion side chain. θ is the dihedral angle between the O—C—C and the C—C—C planes, where O is the connecting oxygen atom to the backbone of the polymer (see inset). The simulated system contains 40 Nafion units, 360 H_2O molecules and 40 H_3O^+ molecules ($\lambda = 10$) at 400 K.

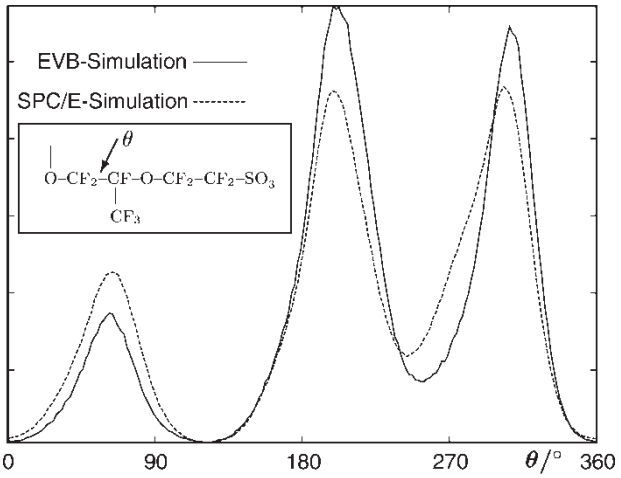

FIGURE 6 Distribution of the torsion angle θ (see Fig. 5) for a simulation with the EVB model (full line) and for a rigid-bond simulation with the SPC/E water model (dashed) at $T = 400$ K and $\lambda = 10$.

correspond to stretched and folded conformations of the side chain. Life times of the conformations can be of the order of a few nanoseconds. Thus, a direct dynamic influence on proton hops can be ruled out.

In addition to the rigid bond simulations we performed a 1.25 ns simulation using a model without any constraints, i.e. the same flexible EVB model for proton transfer as in the slabs and a flexible force field for the Nafion phase [31] was employed. Figure 6 shows the equilibrium distribution of the same torsional angle for both models, averaged over all side chains. Three different conformations are visible in each curve. Both distributions are rather similar and thus justify the use of the more efficient rigid and non-polarizable model for the investigation of large scale motion of larger entities.

Dynamics of Pore Shapes and Fluctuative Bridging

Full two-phase simulations can also provide information about the time dependence of pore forms, connectivity and, at low water content, the possibility of fluctuative bridging between temporarily isolated clusters. Pore shapes do not change significantly over periods of 20 ns as shown in Fig. 7, which shows the initial and final water pore from the 23 ns simulation.

Thus, such simulations need to be run in excess of 100 ns. Furthermore, larger system sizes are needed in order to access the distribution of pore sizes and shapes, and, as suggested by Gierke *et al.*, [4], allow the formation of several water domains and micelles without the restriction of periodic boundary conditions. To our knowledge, no such simulations have been performed to date. While some information may be gained in the future from coarser grained

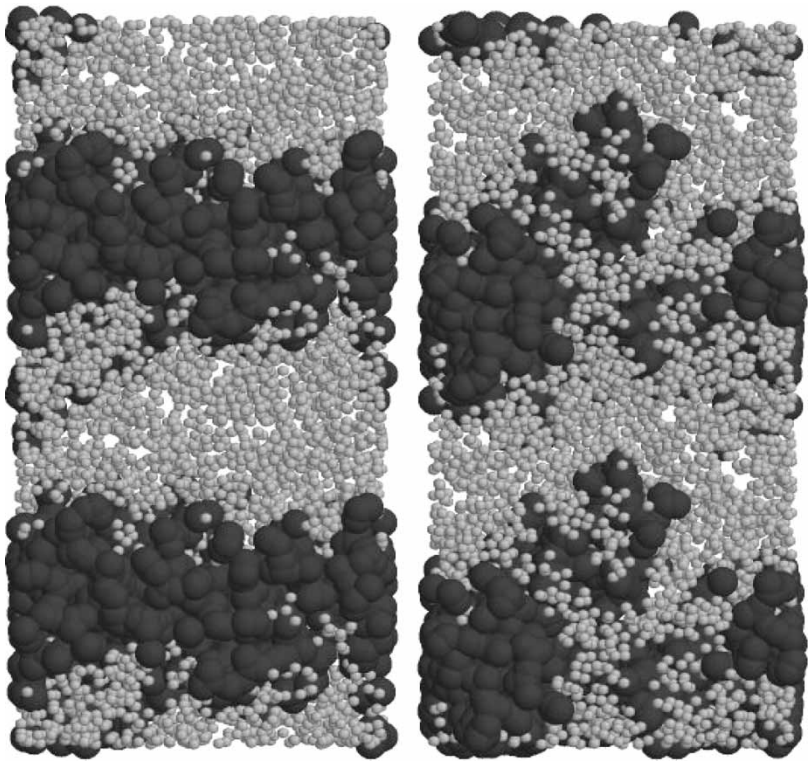

FIGURE 7 Initial (left) and final (right) snapshot of an all-atom simulation of rigid bond-length models of the two-phase system consisting of Nafion and aqueous protonic solution at $T = 400\,\mathrm{K}$ and $\lambda = 5$. Dark grey: aqueous phase; light grey: polymer phase. The initial configuration was chosen as a slab pore. The overall slab-like form is still visible after 23 ns. The basic cubic simulation cell and one of its periodic copies are shown.

models (fused atom models in which CF_n groups are treated as atoms just to mention the most obvious simplification), simulation of a substantial piece of the membrane is almost impossible using molecular models. Approaches from polymer simulation methodology and from percolation theory may be useful in the future.

Water Content Dependence

Depending on the operating conditions of the fuel cell, the water content of the Nafion membrane is not constant across its thickness, which is typically of the order of 100–200 μm. Rather, significant gradients may build up which influence the performance of the cell. At high current output, drying can occur on the anode side of the hydrogen PEM due to co-transport of water with solvated protons (the so-called *electro-osmotic drag*). Without humidification of the hydrogen gas stream this drying can lead to a significant local reduction of conductance as a consequence of the local water dependence of proton conductivity (see above). This is not a problem for the liquid-fed direct methanol fuel cell. In such a cell, however, due to the aforementioned electro-osmotic effect water may condense in the cathode region, which is termed as flooding, and which leads to a reduction of the activity by blocking O_2 access to the catalyst. Local diffusivities as gained from simulations can be used as input to model such inhomogeneities on the continuum mechanics level, an approach that is currently explored in our institute.

Protons Entering and Leaving the Membrane

The investigation by computer simulations of the catalytic steps of anodic proton generation and cathodic proton consumption in a fuel cell with a well-conducting membrane becomes increasingly important under the aspect of optimizing the device. Modeling such steps requires the use of quantum chemical methods, particularly gradient-corrected DFT methods. While such studies are nowadays performed for catalytical gas phase reactions in many groups, the presence of water and polymer phase cannot be neglected in studies relevant for fuel cell operations. Such studies focus on several aspects: the first one is the role of the catalyst composition, whereby different metal alloys can influence the performance and also the economical aspects drastically. Research on the mobility of dissociation and oxidation products of water and methanol (albeit in gas phase and not in the condensed phase) indicates different reactivities in dependence of the relative amounts of the composites [41].

Further aspects are the stabilizing effects of the polar solvent surrounding the reaction products in working fuel cells. Not only the (dissociative) adsorption of methanol or hydrogen but also the stability of intermediates and products might be influenced by the solvent; reaction pathways or side-products, which may not exist at all or not be formed under gas-phase conditions, might become important in the condensed phase. Currently, the adsorption of methanol at the platinum/water interface and the first dehydrogenation step are investigated [42–45]. So far it appears that from the energetic point of view the reaction pathway via initial C—H bond scission is preferable over initial breakage of the O—H bond; in the first case the reaction product can be further stabilized by hydrogen bonds from the solvent to the adsorption products [45]. Furthermore, the dissociation of triflic acid, which can be considered as a model compound for the Nafion head group, has been studied in the presence of water but not in the presence of catalyst by means of *ab initio* simulations [18,19]. Combining the two features in a single system is currently under investigation [45].

SUMMARY

Understanding proton transport in polymer electrolyte membranes on various time and length scales can aid the design and optimization of low temperature fuel cells. Most computer simulation work to date has been performed on the scale of local proton hops in single membrane pores. The influence of several material properties and operational parameters of a fuel cell has been investigated in this way. First, studies on the influence of polymer dynamics on proton transport have been made. Incorporation of the full three-dimensional structure of the pore network and of pore dynamics inside the membrane is, however, still missing in order to bridge the gap between local chemical properties and successful continuum-level descriptions of non-equilibrium transport through the active fuel cell membrane. Quantum chemical calculations of catalytic reactions in the fuel cell environment are still in an early stage of development.

Acknowledgements

Financial support through the "Membranes and Membrane Electrode Assemblies for Direct Methanol Fuel Cells" project supported by the German government under BMWi Grant 0327086 is acknowledged. We would also like to thank the John von Neumann Institute for Computing (NIC) of Forschungszentrum Jülich for computer time.

References

[1] Gottesfeld, S. and Zawodzinski, T.A. (1997) "Polymer electrolyte fuel cells", In: Alkire, R.C., Gerischer, H., Kolb, D.M. and Tobias, C.W., eds, *Advances in Electrochemical Science and Engineering* (Wiley-VCH, Weinheim) **5**, pp 195–301.
[2] Büchi, F.N., Scherer, G.G. and Wokaun, A., eds (2001) *1st European PEFC Forum, 2–6 July, Lucerne, Switzerland* (European Fuel Cell Forum, Oberrohrdorf, Switzerland).
[3] Stolten, D., Emonts, B. and Peters, R., eds (2003) *2nd European PEFC Forum, 30 June–4 July, Lucerne, Switzerland* (European Fuel Cell Forum, Oberrohrdorf, Switzerland).
[4] Gierke, T.D., Munn, G.E. and Wilson, F.C. (1981) "The morphology in nafion perfluorinated membrane products, as determined by wide-angle and small-angle X-ray studies", *J. Polym. Sci. Part B-Polym. Phys.* **19**, 1687–1704.
[5] Dreyfus, B., Gebel, G., Aldebert, P., Pineri, M., Escoubes, M. and Thomas, M. (1990) "Distribution of the micelles in hydrated perfluorinated ionomer membranes from SANS experiments", *J. Phys. (France)* **51**, 1341.
[6] Gebel, G. and Lambard, J. (1997) "Small-angle scattering study of water-swollen perfluorinated ionomer membranes", *Macromolecules* **30**, 7914.
[7] Gierke, T.D. (1977), *J. Electrochem. Soc.* **134**, 319c.
[8] von Grotthus, C.J.D. (1806) "Mèmoiresur la dècomposition de l'eau et des corps qu'elle tien en dissolution à l'aide de l'électricité galvanique", *Ann. Chim.* **LVIII**, 54.
[9] Agmon, N. (1995) "The Grotthuss mechanism", *Chem. Phys. Lett.* **244**, 456–462.
[10] Tuckerman, M., Laasonen, K., Sprik, M. and Parrinello, M. (1995) "*Ab initio* molecular dynamics simulation of the solvation and transport of hydronium and hydroxyl ions in water", *J. Chem. Phys.* **103**, 150.
[11] Tuckerman, M., Laasonen, K., Sprik, M. and Parrinello, M. (1995) "*Ab Initio* molecular dynamics simulation of the solvation and transport of H_3O^+ and OH^- ions in water", *J. Phys. Chem.* **99**, 5749.
[12] Lobaugh, J. and Voth, G.A. (1996) "The quantum dynamics of an excess proton in water", *J. Chem. Phys.* **104**, 2056–2069.
[13] Tuckerman, M.E., Marx, D., Klein, M.L. and Parrinello, M. (1997) "On the quantum nature of the shared proton in hydrogen bonds", *Science* **275**, 817–820.
[14] Marx, D., Tuckerman, M.E., Hutter, J. and Parrinello, M. (1999) "The nature of the hydrated excess proton in water", *Nature* **397**, 601–604.
[15] Marx, D., Tuckerman, M.E. and Parrinello, M. (2000) "Solvated excess protons in water: quantum effects on the hydration structure", *J. Phys.: Cond. Mat.* **12**, A153–A159.
[16] Kreuer, K.D. (1992) In: Colomban, P., ed., *Proton Conductors* (Cambridge University Press, Cambridge), p 474.
[17] Cappadonia, M., Erning, J.W., Niaki, S.M.S. and Stimming, U. (1995) "Conductance of Nafion 117 membranes as a function of temperature and water content", *Solid State Ionics* **77**, 65–69.
[18] Eikerling, M., Paddison, S.J. and Zawodzinski, T.A., Jr. (2002) "Molecular orbital calculations of proton dissociation and hydration of various acidic moieties for fuel cell polymers", *J. New. Mat. Electr. Sys.* **5**, 15–23.
[19] Eikerling, M., Paddison, S.J., Pratt, L.R. and Zawodzinski, T.A., Jr. (2003) "Defect structure for proton transport in a triflic acid monohydrate solid", *Chem. Phys. Lett.* **368**, 108–114.
[20] Paddison, S.J., Eikerling, M., Zawodzinski, T.A., Jr. and Pratt, L.R. (2002) "Molecular modeling of proton conduction in polymer electrolyte membranes of nafion type", *International Conference on Computational Nanoscience and Nanotechnology*, (San Juan, Puerto Rico).
[21] Schmitt, U.W. and Voth, G.A. (1998) "Multistate empirical valence bond model for proton transport in water", *J. Phys. Chem. B* **102**, 5547–5551.
[22] Schmitt, U.W. and Voth, G.A. (1999) "The computer simulation of proton transport in water", *J. Chem. Phys.* **111**, 9361–9381.
[23] Čuma, M., Schmitt, U.W. and Voth, G.A. (2000) "A multi-state empirical valence bond model for acid base chemistry in aqueous solution", *Chem. Phys.* **258**, 187–1999.

[24] Day, T.J.F., Soudackov, A.V., Čuma, M., Schmitt, U.W. and Voth, G.A. (2002) "A second generation multistate empirical valence bond model for proton transport in aqueous systems", *J. Chem. Phys.* **117**, 5839.
[25] Vuilleumier, R. and Borgis, D. (1998) "Quantum dynamics of an excess proton in water using an extended empirical valence-bond hamiltonian", *J. Phys. Chem. B* **102**, 4261–4264.
[26] Vuilleumier, R. and Borgis, D. (1998) "An extended empirical valence bond model for describing proton transfer in $H^+(H_2O)_n$ clusters and liquid water", *Chem. Phys. Lett.* **284**, 71–77.
[27] Krokidis, X., Vuilleumier, R., Borgis, D. and Silvi, B. (1999) "A topological analysis of the proton transfer in $H_5O_2^+$", *Mol. Phys.* **96**, 265–273.
[28] Vuilleumier, R. and Borgis, D. (1999) "Transport and spectroscopy of the hydrated proton: a molecular dynamics study", *J. Chem. Phys.* **111**, 4251–4266.
[29] Walbran, S. and Kornyshev, A.A. (2001) "Proton transport in polarizable water", *J. Chem. Phys.* **114**, 10039–10048.
[30] Warshel, A. and Weiss, R.M. (1980) "An empirical valence bond approach for comparing reactions in solutions and in enzymes", *J. Am. Chem. Soc.* **102**, 6218.
[31] Spohr, E., Commer, P. and Kornyshev, A.A. (2002) "Enhancing proton mobility in polymer electrolyte membranes: lessons from molecular dynamics simulations", *J. Phys. Chem. B* **106**, 10560–10569.
[32] Commer, P., Cherstvy, A.G., Spohr, E. and Kornyshev, A.A. (2002) "The nature of water content effect on the proton transport in polymer electrolyte membrane", *Fuel Cells* **2**, 127–136.
[33] Kornyshev, A.A., Kuznetsov, A.M., Spohr, E. and Ulstrup, J. (2003) "Kinetics of proton transport in water", *J. Phys. Chem. B* **107**, 3351–3366.
[34] Kreuer, K.D. (1997) "On the development of proton conducting materials for technological applications", *Solid State Ionics* **97**, 1–97.
[35] Eikerling, M. and Kornyshev, A.A. (2001) "Proton transfer in a single pore of a polymer electrolyte membrane", *J. Electroanal. Chem.* **502**, 1–14.
[36] Vishnyakov, A. and Neimark, A.V. (2001) "Molecular dynamics simulation of microstructure and molecular mobilities in swollen nafion membranes", *J. Phys. Chem. B* **105**, 9586–9594.
[37] Spohr, E. (2004) "Molecular dynamics simulations of proton transfer in a model nafion pore", *Mol. Simul.* **30**, 107–115.
[38] Seeliger, D., Hartnig, C. and Spohr, E. (2004) in preparation.
[39] Berendsen, H.J.C., Grigera, J.R. and Straatsma, T.P. (1987) "The missing term in effective pair potentials", *J. Phys. Chem.* **91**, 6269.
[40] Fornili, S.L., Migliore, M. and Palazzo, M.A. (1986) "Hydration of the hydronium ion. *Ab Initio* calculations and Monte carlo simulations", *Chem. Phys. Lett.* **125**, 419.
[41] Shubina, T.E. and Koper, M.T.M. (2002) "Quantum-chemical calculations of CO and OH interacting with bimetallic surfaces", *Electrochim. Acta* **47**, 3621.
[42] Mattson, T.R. and Paddison, S.J. (2003) "Methanol at the water-platinum unterface studied by *ab initio* molecular dynamics", *Surf. Sci.* **544**, L697–L702.
[43] Greeley, J. and Mavrikakis, M. (2002) "A first-principles study of methanol decompsition on Pt(111)", *J. Am. Chem. Soc.* **124**, 7193–7201.
[44] Okamoto, Y., Sugino, O., Mochizuki, Y., Ikeshoji, T. and Morikawa, Y. (2003) "Comparative study of dehydrogenation of methanol at Pt(111)/water and Pt(111)/vacuum interfaces", *Chem. Phys. Lett.* **377**, 236–242.
[45] Hartnig, C. and Spohr, E., unpublished results.